

# ASTOS 8.1 - MISSION PERFORMANCE ANALYSIS, SYSTEM CONCEPT ANALYSIS AND OTHER NEW FEATURES

Sven Weikert<sup>(1)</sup>, Alexander Dobler<sup>(1)</sup>, Jochen Teufel<sup>(1)</sup>, Sven Schöff<sup>(1)</sup>, Valentino Zuccarelli<sup>(1)</sup>,  
 Martin Jürgens<sup>(1)</sup>, Andreas Wiegand<sup>(1)</sup>, Sven O. Erb<sup>(2)</sup>

(1) Astos Solutions GmbH, (2) European Space Agency, ESTEC

## ABSTRACT

This paper presents the main extensions of ASTOS incorporated into release 8.1. First it gives an overview on ASTOS and its workflow, then it presents the new capabilities. Four new major developments have been made for the release 8.1 of ASTOS focusing on new markets and increased usability:

- An integrated set of mission performance analysis features that cover almost all aspects required to fill a mission analysis report according to DOPS-GS-RM-1002-OPS-OSA.
- Models and techniques for system concept analysis considering the power system, thermal control system as well as data management and communication systems
- A built-in tool to import CAD models, to easily texturize them and to use them for the built-in animation tool
- New wizards that ease the set-up of an ASTOS scenario and that help migrating a scenario from one to another application.

The paper details on each of the above mentioned new functionalities, showing user input and results taken from typical example scenarios.

## 1. ASTOS OVERVIEW AND WORKFLOW

With ASTOS it is possible to set up arbitrary space scenarios with multiple vehicles (also constellations), ground stations, areas of interest and points of interest. Each vehicle or station may consist of several elements like sensors, actuators (like thrusters, torquers or wheels), tanks, structural components, batteries, solar generators, radiators, etc.

A set of customizable models with various complexity and realism is available for each of the abovementioned categories (model database). The same for environmental models like atmosphere, gravity field, magnetic field, hydrosphere, ephemerides and celestial body spin models.

Ones configured, all these models can be reused throughout the scenario (template approach). Via a graphical “Vehicle Builder” a spacecraft or rocket can be built from the defined and configured elements, whereas the element’s aspects like positioning, their role or contribution in the power, thermal control or data management system or their

graphical representation (e.g. for animations) can be configured.

Via the dynamics configuration, initial states and the translational and rotational motion of each vehicle can be defined (e.g. equations of motion, attitude control laws; 3-dof or 6-dof propagation), whereas motion rules can be changed throughout the simulation time (multi-phase concept).

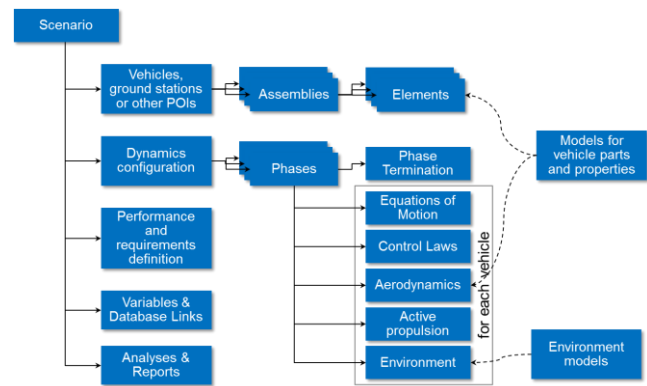


Figure 1: ASTOS scenario overview

The further work flow of ASTOS depends on the application: It might consist just of a simulation and results inspection (by means of the built-in plotting and animation tools or using one of the available export filters), but it can be more complex e.g. if the optimization or batch processing feature of ASTOS is used (see Figure 2).

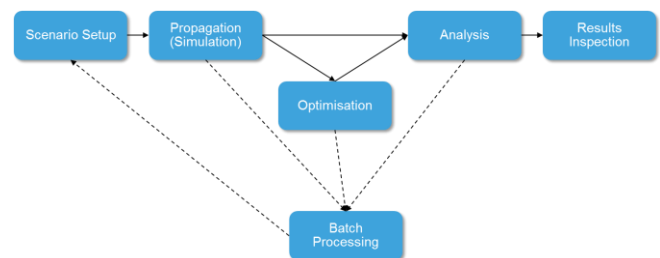


Figure 2: ASTOS workflow

Several hundred output functions are provided already in a standard ASTOS simulation output file. However, further information can be exploited from the simulation result in

post-processing step by means of a variety of available analyses. Such analyses are described below.

## 2. MISSION PERFORMANCE ANALYSIS

The ASTOS software tries to cover all mission performance aspects that can be assessed by means of analysis software. With ASTOS 8.1 these mission performance aspects can be analyzed with ASTOS:

- eclipses
- fuel budget and operational life-time
- end-of-life disposal
- ground station coverage
- electrical power budget
- data management and storage
- orbit evolution

Since coverage analysis and orbit evolution are covered already by previous releases of ASTOS 8, they are not addressed by this paper. Electrical power budget as well as data management and storage are aspects that are explained in chapter 3.

### 2.1. Lifetime Prediction

The lifetime prediction analysis of ASTOS calculates the fuel consumption due to various maneuvers:

- insertion correction
- orbit keeping
- attitude correction and desaturation of wheels
- collision avoidance maneuvers
- deorbitation or graveyarding

Based on the user-defined fuel and requested fuel margin the operational life-time is calculated.

The life-time prediction is based on simple assumptions and empirical formulations so that a full closed-loop model of the AOCS system is not required to run the analysis and to obtain results. A long-term simulation is also not required. First the required fuel for the disposal maneuver is calculated. For de-orbit maneuvers the following formula is used to calculate the required velocity change ( $\Delta V$ ):

$$\Delta V_{deorbit} = \sqrt{\mu \left( \frac{2}{r_{apo}} - \frac{1}{a} \right)} - \sqrt{2\mu \left( \frac{1}{r_{apo}} - \frac{1}{r_{apo} + r_{deorbit}} \right)}$$

whereas  $r_{deorbit}$  is the user-defined perigee radius after the deorbit maneuver. For GEO orbits a Hohmann transfer into the following graveyard altitude is considered:

$$h_{graveyard} = h_{GEO} + 235km + (1000C_R A/m)$$

whereas  $C_R$  is the solar radiation pressure coefficient,  $A$  the reference area and  $m$  the dry mass. Based on the user-defined

Isp the fuel consumption for the deorbit maneuver is calculated and subtracted from the overall fuel. For orbit types different from those mentioned above, the user has to specify a fuel budget for disposal maneuvers.

The remaining fuel is used to calculate the operational life-time. In case of repeating ground-tracks the algorithms described in [1] are applied (algorithms 71 and 72).

For geostationary orbits luni-solar perturbations are considered in accordance with [2]:

$$\Delta V_{Moon} = 102.67 \cos \alpha \sin \alpha$$

$$\Delta V_{Sun} = 40.17 \cos \gamma \sin \gamma$$

whereas  $\alpha$  is the angle between the orbit plane and the Moon orbit and  $\gamma$  is the angle between the orbit plane and the ecliptic.

Further the  $J_{22}$ -effect, causing East-West drift is considered as follows:

$$\Delta V_{J22} = 1.715 |\sin(2(l_D - l_S))|$$

whereas  $l_D$  is the required longitude and  $l_S$  is the closest stable longitudinal position, which is either  $75^\circ$  or  $255^\circ$ . To be noted that all velocity increments are given in m/s per year.

In order to consider  $\Delta V$  required to compensate orbit decay due to atmospheric drag, the reduction of the semi-major axis per revolution is assumed as

$$\Delta a_{rev} = -2\pi(C_D A/m)a^2\rho_p \exp(-c)(I_0 + 2eI_1)$$

and the reduction of eccentricity is assumed as:

$$\Delta e_{rev} = -2\pi(C_D A/m)a\rho_p \exp(-c) \left( I_1 + \frac{e}{2}(I_0 + I_2) \right)$$

with

$$c \stackrel{\text{def}}{=} a e/H$$

whereas  $I_0$ ,  $I_1$  and  $I_2$  are modified Bessel functions with argument  $c$ ;  $H$  is the density scale height, and  $\rho_p$  is the density at perigee.  $C_D$  is assumed to be 2.2.

Based on these formulations and user-specified thresholds for semi-major and eccentricity errors, the frequency of correction maneuvers is calculated. Every time the threshold is reached a correction comprising two impulsive maneuvers are considered.

In order to consider collision avoidance maneuver, the user has to specify the debris flux (number of debris crossing a reference area for each size class) as it is provided e.g. by the MASTER software [3] and the position uncertainty for each size class.

Further the position uncertainty of the vehicle and the accepted collision probability is user-provided. From this the

collision cross-section is calculated, which gives - together with the debris flux - directly the mean time between two collision avoidance maneuvers (for the given debris size class). In-track correction maneuvers are assumed calculating the required velocity increment and fuel consumption.

It is also possible to include launcher dispersion and an orbit transfer from launch orbit to mission orbit. This includes the following corrections:

- Semi-Major Axis  $a$  and Eccentricity  $e$ : corrected together with two-impulsive maneuvers at apogee and perigee
- Inclination  $i$ : the inclination change is performed at the ascending node. The delta-V is calculated as:

$$\Delta V = 2 * v_{asc} * \sin\left(\frac{1}{2} * \Delta i\right)$$

- Right ascension: the right ascension of the ascending node  $\Omega$  is corrected at the maximum latitude point, i.e. the greatest distance from the equatorial plane:

$$\Delta V = 2 * v * \sin(i) * \sin\left(\frac{1}{2} * \Delta \Omega\right)$$

- Argument of Periapsis  $\omega$  the argument of periapsis is changed with two impulsive maneuvers at eccentric anomaly  $E$  of  $90.0^\circ$  and  $270.0^\circ$ .

$$\Delta V = |\Delta \omega| \frac{n a e}{\text{Sqrt}(1 - e^2) + \sin(|E|)}$$

$$\Delta a = \Delta V * 2a * \frac{\text{Sqrt}(1 - e^2)}{n * r}$$

- True anomaly  $\theta$ : the phasing is achieved by lowering the orbit altitude to a phasing orbit with period  $P$  and semi-major axis  $a$  as follows:

$$P_{phasing} = \frac{2\pi - \frac{\Delta \theta}{num_{phasingRevs}}}{n_{orig}}$$

$$a_{phasing} = \left( P_{phasing} * \frac{\text{Sqrt}(\mu)}{2\pi} \right)^{\frac{2}{3}}$$

With  $n$  being the mean motion of the orbit,  $r$  the radius of the vehicle,  $num_{phasingRevs}$  the user specified number of phasing revolutions.

All applicable velocity increments are summed and the  $I_{sp}$  and vehicle mass is used to calculate the fuel consumption within a given time span, whereas the vehicle mass is updated after every maneuver.

## 2.2. Automatic Report Generation

In order to reduce the effort for the user, ASTOS can create automatically generated reports that can be customized by the user. For the mission performance analysis a report is generated that follows a structure as it is defined in the ESA Mission Analysis Guidelines for Earth Observation Missions [4]. All sections and paragraphs of the report will be filled by ASTOS as far they are related to analyses results or user-provided input. The report function can collect the results from several different analyses and scenarios such that all mission phases (insertion, LEOP, operations, disposal) can be considered.

The report can be either generated as Microsoft Word document or as an HTML website. Customization can be performed at two stages: either on template level, i.e. the customization is considered every time a report generation is initiated (e.g. after input data was modified), or by modifying the report document (Word or HTML). Customization capabilities of the report include also the global document layout such that the company CI and document standards can be followed.

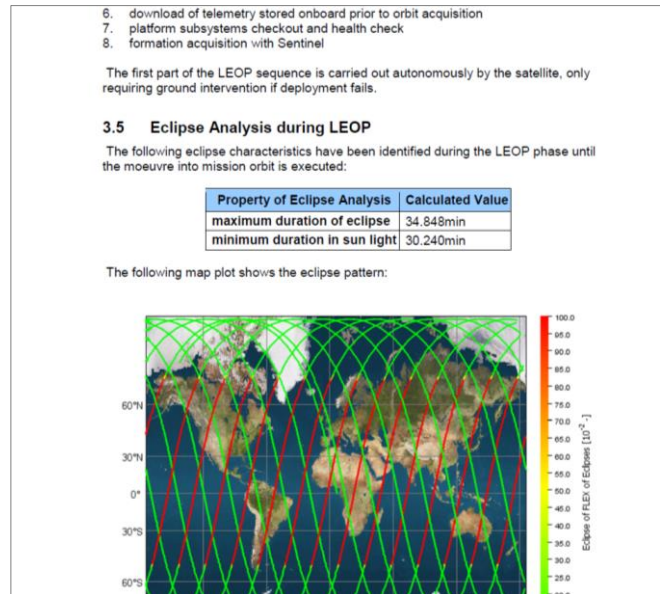


Figure 3: Excerpt from an automatically created mission analysis report

## 3. SYSTEM CONCEPT ANALYSIS

The system concept analysis feature of ASTOS 8.1 allows preliminary design and performance analysis of the power, the thermal control and data management systems of an orbital spacecraft. This new functionality is seamlessly integrated into ASTOS, i.e. each definable element of the

scenario has now optional parameters that characterize their behaviour under thermal, power or data aspects (e.g. heat production or power consumption). These generic elements are accomplished by new models dedicated to system concept analysis (e.g. batteries, solar arrays, data storages, radiators). Each system is defined by means of a node model, i.e. elements, representing nodes, can be connected to a system. Node connections can be defined via a connection table, whereas connections can be controlled by means of a graphical representation (see Figure 4).

In the following paragraphs the model and assumptions for each subsystem is presented.

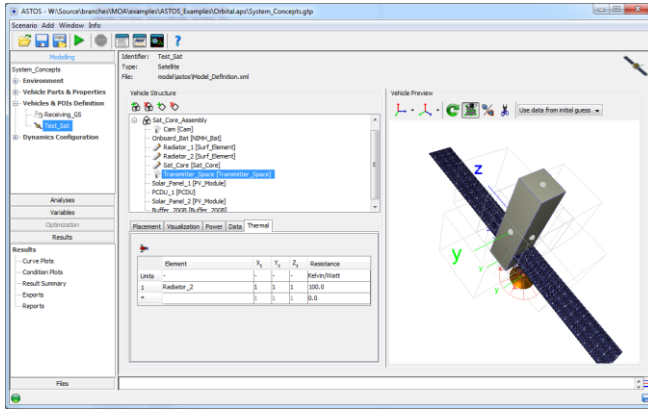


Figure 4: Node definition and graphical representation

### 3.1. Thermal (Control) System Model

The thermal system model shall provide information on the temperature evolution of individual satellite components. It shall further provide information on generated and radiated heat. Each element of the spacecraft represents a thermal node; surface elements (radiators) have a user-defined number of thermal nodes.

#### 3.1.1. Heat Transfer and Nodal Temperatures

The heat conduction between two thermal nodes is governed by their connection's user-defined thermal resistance  $R_{th}$  and the temperature drop  $\Delta T$  between these two thermal nodes:

$$\dot{Q} = R_{th}\Delta T$$

The temperature state is integrated using the user-defined initial temperature and the state derivative:

$$\dot{T} = mc_p \sum_{i=1}^n \dot{Q}_i$$

whereas  $m$  is the mass and  $c_p$  the specific heat capacity of the thermal node.

#### 3.1.2. Surface Irradiation and Emission

First the angle between the vector towards the sun and the normal of each irradiation surface is calculated (including radiator surfaces). For surfaces, where this angle is less than  $90^\circ$ , the irradiated power is calculated. This power depends on the projected area  $A_{proj}$ , the distance to the sun  $r$  and the emissivity  $\epsilon$  of the surface material:

$$\dot{Q}_{irr} = A_{proj}\epsilon \frac{\Phi}{4\pi r^2}$$

whereas  $\Phi$  is the radiation power of the sun, which is assumed to be  $3.845 \cdot 10^{26}$  W.

As mentioned above, surface elements are also thermal nodes with their own temperature. Based on this temperature the radiated power is calculated using the Stefan-Boltzmann law:

$$\dot{Q}_{rad} = A\epsilon\sigma T^4$$

whereas  $A$  is the area of the surface element,  $\sigma$  is the Stefan-Boltzmann constant and  $T$  is the temperature of the surface. Heat transfer between surface elements is calculated using a 2D heat conduction formulation.

The model considers eclipses due to all present celestial bodies. Self-shadowing and shadowing by other spacecrafts is not considered. Irradiation between surface elements and other components of the satellite is not considered as well.

### 3.2. Power System Model

The power system model shall provide an estimate of the power state and consumption over time. As mentioned above it provides models for batteries and power generators. Further each equipment model has an optional power consumption definition.

In ASTOS 8.1 the user can define several circuits and their voltages via a virtual PCPU to which consumers, producers and batteries can be connected. A positive budget results in charging of connected batteries, while negative budgets result in a discharge of the batteries.

#### 3.2.1. Battery Model

Batteries are modelled according to [5]. This model defines the battery voltage depending on the charge/discharge current and the remaining capacity for various technologies including the hysteresis behavior when approaching the fully charged state. The applied current is the state derivative of the capacity and further output of this model include the state-of-charge as well as provided electrical power.

Since batteries are often build from several cells, the number of cells in series and/or in parallel is a user input for this model. The other input parameters can be easily extracted from data sheets provided by the manufactures. The filtered current  $i^*$  in the formulations of Tremblay (first-order low-pass filter with 30s time constant) is assumed to be equal to the battery current. This is possible since high-frequent load changes are not modelled.

### 3.2.2. Solar Generators

Solar generators are modelled according to [6]. First the solar irradiation is calculated based on the size of the panel, the angle between its normal vector and the vector towards the sun, the distance to the sun and the occurrence of eclipses.

From the irradiation, the parameters of the photovoltaic elements and its temperature, the maximum power voltage and the output current are calculated.

### 3.3. Communication & Data System Model

Large amount of (scientific and telemetry) data is usually produced on board by different sources. This data is stored in dedicated hardware while waiting to be transferred to ground, since a link cannot be established at any time.

The communication and data model shall provide the data rates, the amount of stored data and the transfer delay in a communication chain. The ASTOS model considers two parts: the generation, transmission and storage of data within the spacecraft and the transmission of data to and from other spacecrafts or ground stations.

Each element of the spacecraft can be defined as data provider (e.g. housekeeping data). The data produced by sensors depends on their type and switching condition (sensors can be automatically deactivated based on certain conditions like eclipses).

#### 3.3.1. Radio Signal Propagation and Link Budget

Once the electromagnetic wave leaves the transmitter, it has still to travel long before reaching the receiver. During this phase, the signal has to go through many different sources.

The main loss is caused by the propagation itself (free space loss). Losses in the signal also occur due to the presence of the atmosphere. Especially in the troposphere several effects have to be considered, as for instance the effect of meteorological phenomenon as rain, clouds and fog; and the effect that some gasses such as oxygen and water vapor have on the signal and scintillation. All these losses are modelled according to [7].

The link budget accounts for all gains and losses when sending an electromagnetic signal from a source transmitter (Tx), to a target receiver (Rx). All what “increases” the transmitted signal/power is defined as gain, as those produced by antennas. The following antenna models are implemented: isotropic, parabolic, axial helix, horn and dipole. On the other

hand, all what “decreases” the transmitted power is defined as loss, which can take place at the Tx or at the Rx (e.g. thermal noise, cable losses, etc) or during the propagation of the signal through the medium (e.g. free space and atmospheric attenuation).

The main objective of the link budget is to compute the received power at the Rx, which assesses the quality of the signal after the propagation and tells whether data can be transferred. The signal-to-noise ratio (SNR) is one of the key parameters computed in order to evaluate the quality of the link. It is the ratio between the received power and the noise power at the receiver in a given bandwidth.

The equivalent isotropic radiated power (EIRP) computation represents the main positive contribution to the SNR and it depends on the Tx characteristics (power and gain). The G/T (gain to temperature noise ratio) computation contains a positive contribution, due to Rx gain and a negative contribution due to the noise at the receiver. The main negative term is caused by the propagation losses. The  $K_{Pol}$  and  $K_B$  coefficients (whose values are between 0 and 1) account for the mismatch of polarization and bandwidth respectively.

The received power  $P_r$  and the noise power  $N_0$  at the receiver can be expressed as:

$$P_r = \frac{EIRP \cdot G_r}{L} K_{Pol} K_B$$

and

$$N_0 = KT_{Sys}B$$

where  $G_r$  is the gain of the receiver,  $T_{Sys}$  is the receiver noise temperature,  $B$  is the bandwidth,  $L$  is the total signal loss and  $K$  is the Boltzmann constant.

Since the SNR is defined as the ratio between the received and noise power at the receiver, the mathematical relation can be derived (as a linear power ratio, not as logarithmic decibels):

$$SNR = \frac{P_r}{N_0} = \frac{EIRP \cdot G/T}{L \cdot KB} K_{Pol} K_B$$

Another important figure of merit is the CNR, defined as the received and the noise power at the receiver per unit bandwidth and it is usually expressed in dB-Hz. The relation between SNR and CNR is provided by:

$$CNR = SNR + 10 \log_{10} B$$

### 3.3.2. Data storages

Data storages can buffer the data produced by spacecraft elements or received by sensors. They are specified by their capacity and treated as FIFO buffers (first-in-first-out). Within a post-processing step it is further possible to analyze the delay of data transmission caused by the buffering process, i.e. it is possible to determine the age of data when it received by a ground station.

## 4. CAD IMPORT AND TEXTURING TOOL

The visualization tools of ASTOS 8.1 require a triangle mesh of all vehicles which should be visualized. A good source for such meshes are CAD models. A common file format for CAD models is STEP (*STandard for the EXchange of Product model data*). Unfortunately, this file format cannot store material (surface) information required by the visualization tools of ASTOS 8.1 (e.g. the animation window *Astroviev*). Therefore a pre-processing step is required in order to apply the material properties to the raw meshes. Also a conversion from STEP to the Wavefront OBJ file format is required in order to use the meshes inside ASTOS.

Available standard tools like Blender are complex to use, especially for an inexperienced user. Therefore, ASTOS 8.1 offers a new tool called the CAD Import and Texturing Tool. This tool enables the user to apply material properties like diffuse surface reflection as well as material textures to a CAD model imported from STEP files. It does not require deep knowledge of 3D modelling, which also enables inexperienced users to pre-process meshes. Additionally, this tool provides an export to the Wavefront OBJ file format.

The CAD Import and Texturing Tool provides a list of predefined materials which already contain the correct material properties and appropriate textures if required. The user simply has to select the surface and the predefined material in order to apply it to the mesh. Most of the algorithms used by the CAD Import and Texturing Tool are common algorithms used in the field of computer graphics. For ASTOS 8.1, they are slightly simplified in order to give also inexperienced users the possibility to apply them on virtual surfaces successfully.

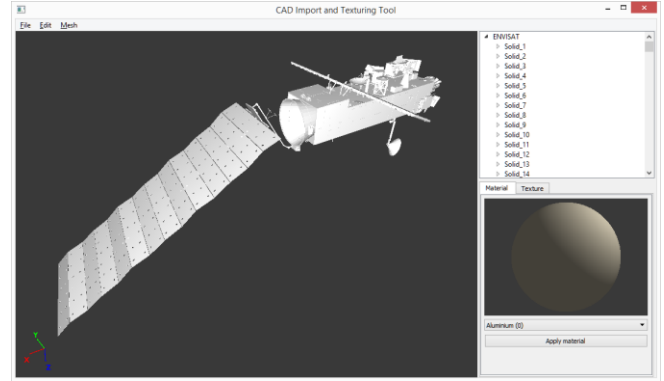


Figure 5: Untextured model as imported from CAD

A common problem of standard texturing methods is that applying a texture to a surface suffers from image distortion.

For the CAD Import and Texturing Tool the reduced length distortion mapping was developed. It is based on the *Angle Based Flattening* algorithm (ABF) described by Sheffer and de Sturler [8]. The purpose of this algorithm is to reduce the image distortions as much as possible without any user interaction. The *Angle Based Flattening* algorithm consists of two parts. In the first part, a constrained minimization problem is solved. The solution of the constrained minimization problem is a mapping from the three-dimensional surface domain to the two-dimensional parametric domain with minimized angle distortion. The second part computes a second mapping from the two-dimensional parametric domain to the two-dimensional parametric domain, which tries to minimize the length distortion.

The algorithm used for ASTOS 8.1 focuses on small time consumption and no user interaction. Because the first part of the ABF algorithm takes a lot of time for solving a system of several thousand linear equations, it is replaced by a simple mapping, e.g. a spherical mapping in order to generate the initial texture coordinates in the parametric domain. The second part of the ABF algorithm is used without any modifications. Therefore, the algorithm used in ASTOS 8.1 only tries to minimize length distortions.

For the minimization of the length distortion, a mapping  $g: \mathbb{R}^2 \rightarrow \mathbb{R}^2$  needs to be defined. For the computation of this mapping, Laplacian grid smoothing is used for its simplicity. Let  $V$  be the set of all vertices and  $E$  the set of all edges of the mesh. First of all, a sizing function representing the isotropic distortion ratio is computed as follows

$$R_{k,l} = \frac{2D\|e\|}{3D\|e\|}, \forall e = (v_k, v_l) \in E, v_i \in V$$

Afterwards, for all vertices  $v_i \in V$ , the normalized average distortion ratio  $\tilde{R}_i$  is computed as the average distortion of all edges  $e$  connected to  $v_i$ .

$$\tilde{R}_i = \frac{1}{|\{e\}|} * \sum_e \left( \frac{2D\|e\|}{3D\|e\|} - 1 \right)^2$$

The distortion of every surface point  $p$  is then defined by using the barycentric coordinates of  $p$ . In order to compensate the length distortions introduced by the initial projection  $S(p)$ ,  $g$  needs to be roughly equal to  $S^{-1}(p)$ .  $g$  is computed by first computing  $g^{-1}$  and inverting it. Initially, a uniform Cartesian grid  $G_1$  is created based on the bounding box of the projected triangle mesh. Laplacian grid smoothing is then applied in order to generate a second grid  $G_2$ . Finally, the mapping from  $G_1$  to  $G_2$  is equal to  $g^{-1}$ . The final texture coordinates are computed by mapping points from  $G_2$  to  $G_1$ . Another problem of standard texturing methods is, that no physical sizes are associated with a texture image. Even if the CAD Import and Texturing tool provides scaling transformations for texture coordinates, it is quite hard to find the correct settings in order to map the texture image physically correct. Therefore, the CAD Import and Texturing Tool uses a material library which provides physical sizes for texture images used by the predefined materials. These physical sizes are later used by the various projections in order to compute physically correct texture coordinates. This step contains a simple texture coordinate scaling based on the model size and the physical size defined for the applied texture.

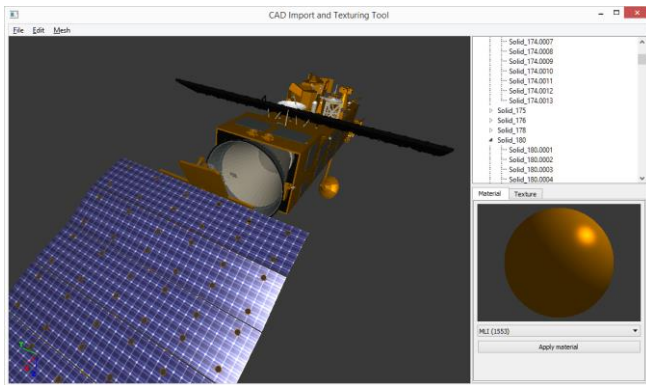


Figure 6: Textured model, ready for visualization

Using the CAD Import and Texturing Tool, it is also possible to apply a logo image on top of a surface with an assigned material. Because the Wavefront OBJ file format does not support multi-texturing, special actions are required in case the applied material is using a texture. In this case the image of the material texture and the logo image are combined into

one single image during the Wavefront OBJ file export. Because the logo is initially defined in the same texture coordinate space as the material texture, this can be easily done.



Figure 7: Astroviev animation window of ASTOS 8.1 showing a textured satellite

## 5. WIZARDS

ASTOS is a very versatile and powerful tool. Therefore it is intelligible that extensive training is need to effectively utilize all features of ASTOS.

In order to reduce the effort required to set up a scenario, a wizard system has been introduced with ASTOS 8.1. By means of questions addressing the desired application, mission phase and spacecraft parameters the wizard system will set up a preconfigured scenario. This is helpful not only for beginners but it reduces also the effort for expert users who – before ASTOS 8.1 – typically started from an existing scenario to avoid building a scenario from scratch. This wizard system allows further to modify an existing scenario, e.g. to convert an optimization application into a reference guidance scenario. Which requires several steps if done by hand.

## 6. OTHER NEW FEATURES

Besides the abovementioned developments ASTOS 8.1 provides many other new features that are briefly listed below:

- Initial state definition as Lissajous or HALO orbit
- Propagation as circular restricted three-body problem
- Consideration of relativistic effects and solar-radiation pressure for long-term propagation
- Instantaneous maneuvers for interplanetary trajectories (injection and correction maneuvers)
- Pork-chop plots

## 7. CONCLUSION

The release 8.1 significantly extends the capabilities of the ASTOS software and opens new markets for a software that started as an optimization tool for launcher trajectories more than 20 years ago. Nowadays ASTOS is able to perform design optimization, mission performance, system concept and safety analysis tasks.

In order to mitigate the risk that the complexity of the tool impedes its usability, measures like the introduction of a wizard system were taken.

## 8. REFERENCES

- [1] Vallado, D.A., *Fundamentals of Astrodynamics and Applications*, Springer, The Netherlands, 2007
- [2] Larson, W.J., Wertz, J., *Space Mission Analysis and Design*, Second Edition, Microcosm, USA, 1992
- [3] ESA MASTER software (Meteoroid and Space Debris Terrestrial Environment Reference), <https://sdup.esoc.esa.int/web/csdtf/home>
- [4] Pellón Bailón, J.-L., *Mission Analysis Guidelines for Earth Observation Missions*, European Space Agency, 2005
- [5] Tremblay, O., Dessaint, L.-A., *Experimental Validation of a Battery Dynamic Model for EV Applications*, World Electric Vehicle Journal Vol. 3, Stavanger, Norway, May 13 - 16, 2009
- [6] Pandiarajan, N., Muthu, R., *Mathematical Modeling of Photovoltaic Module with Simulink*, International Conference on Electrical Energy Systems (ICEES 2011), 3-5 January 2011
- [7] ITU-R P.618-10, *Propagation data and prediction methods required for the design of Earth-space telecommunication systems*, 10/2009
- [8] Sheffer, A., de Sturler, E., *Non-Distorted Texture Mapping Using Angle Based Flattening*, <http://www.math.vt.edu/people/sturler/Publications/UIUCDCS-R-2001-2257.pdf>